William R. Wiley
EMSL
Environmental Molecular Sciences Laboratory

EMSL Report

October – November 2006

The W.R. Wiley Environmental Molecular Sciences Laboratory (EMSL) is a U.S. Department of Energy (DOE) national scientific user facility located at Pacific Northwest National Laboratory (PNNL) in Richland, Washington. EMSL is operated by PNNL for the DOE Office of Biological and Environmental Research. At one location, EMSL offers a comprehensive array of leading-edge resources in six research facilities.

Access to the capabilities and instrumentation in EMSL facilities is obtained on a peer-reviewed proposal basis, and users are participants on accepted proposals. EMSL staff members work with users to expedite access to the facilities and the resident scientific expertise. The bimonthly report documents research and activities of EMSL staff and users.

Research Highlights

Imaging Water Dissociation on TiO_2(110): Evidence for Inequivalent Geminate OH Groups

Z Zhang,[(a)] O Bondarchuk,[(b)] BD Kay,[(a)] JM White,[(b)] and Z Dohnálek[(a)]

(a) Pacific Northwest National Laboratory, Richland, Washington
(b) University of Texas at Austin, Austin Texas

Titania (TiO_2) is widely used as a catalyst and may provide a pathway for the use of solar radiation as a viable source of clean energy. Understanding the chemical activity of this material has become the focus of a number of model catalytic studies, and these results are a major step towards that direction.

The TiO_2-H_2O system is of great interest for many areas of both fundamental and applied science, including the areas of photo-catalysis, electrochemistry, active coatings, and corrosion. For example, the discovery of photochemical water dissociation on TiO_2, with potential applications in solar cells, has stimulated extensive research on reactions of water on TiO2 surfaces. In particular, the detailed understanding of water adsorption, diffusion, and dissociation on prototypical rutile TiO_2(110) has become one of the leading topics in the area of oxide surface chemistry. The reactivity of rutile TiO_2(110) is believed to be dominated by missing oxygen ion defect sites, generally called bridge-bonded oxygen vacancies (BBO_V). There is good evidence that dissociative adsorption is limited to BBO_V sites. Understanding the chemical activity of this particular surface site has become the focus of a number of model catalytic studies.

Scanning tunneling microscopy (STM) makes it possible to image the adsorption, dissociation, and diffusion of atoms and molecules on surfaces. We used STM to image and characterize the time evolution of hydroxyl (OH) groups formed upon H_2O dissociation on TiO_2(110) BBO_V sites at very low coverage. Figure 1 shows STM images of the same surface area before (a) and after (b) background adsorption of H_2O at room temperature. The bright rows in Figure 1 are identified as the fivefold coordinated Ti^{4+} ions; the dark rows are the BBO ions. The bright spots along

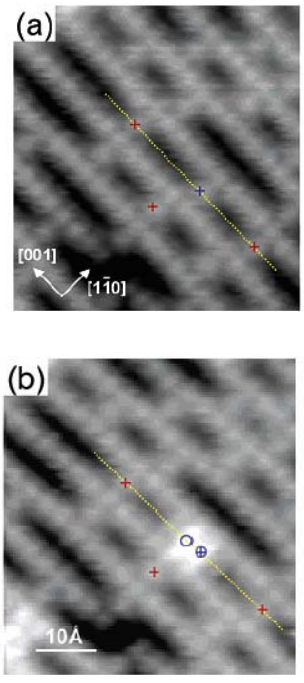

Figure 1. Two STM images obtained from the same area of TiO_2(110) before (a) and after (b) background adsorption of H_2O at room temperature. The + signs mark the positions of several BBO_Vs. Two circles mark the positions of two OH groups formed after H_2O adsorption and dissociation on the BBO_V site.

the BBO rows are assigned to BBO_Vs. Figure 2 shows line scans along dark rows in the images in Figures 1a and 1b. In Figure 2, the vertical dashed gridlines correspond to the positions of the BBO atoms. The two curves in Figure 2 are line scans of identical segments along the [001] direction before and after dosing water from the background. Two of the three vacancies on the dotted line in Figure 1(a) remain unoccupied in Figure 1(b), while the third vacancy is replaced by a broader, higher-intensity region with two local maximas. The positions of the two local maxima provide direct evidence that water molecules dissociate upon adsorption on BBO_Vs at 300 K. Our results confirm that paired hydroxyl groups are the direct product of water dissociation on oxygen vacancies.

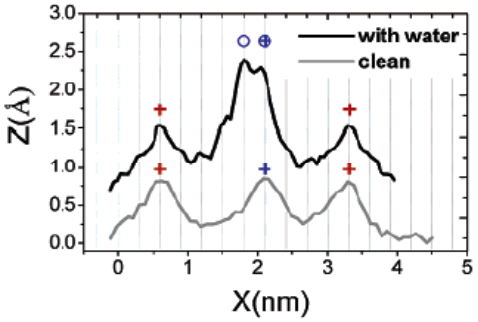

Figure 2. Line profiles indicated in Figure 1 panels (a) and (b) before and after water adsorption along the [001] direction. Vertical lines represent the bridge-bonded oxygen atom positions.

In subsequent images, we tracked the OH groups as a function of time. This experiment provides valuable insight because the positions of the original BBO_Vs are known. For the first time, the hydrogens of these hydroxyl pairs are found spontaneously separated along the (001) direction, indicating hydrogen hopping without the assistance of water molecules. Surprisingly, we found that the hydrogens of the hydroxyl pair are not identical; the first hydrogen hop is much less likely for the hydrogen located at the original vacancy. That is, the first hop associated with the nearest-neighbor hydroxyl pair formed from H_2O dissociative adsorption strongly favors motion of the hydrogen on OH_B. This observation is rather puzzling considering the generally accepted view of equivalent OH groups formed by water dissociation. Therefore, we would expect that, upon OH pair formation, the charge should redistribute and lead to formation of a symmetric OH pair. Our experiments clearly indicate that this is not the case, and that the electronic environment of these two OH groups is likely different.

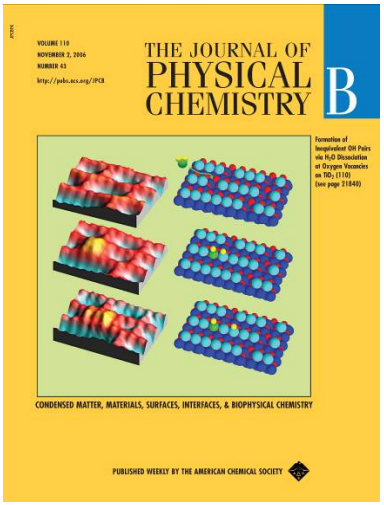

Figure 3. November 2, 2006, issue of *The Journal of Physical Chemistry B*.

This exciting work was featured on the cover of the August 31, 2006, issue of *The Journal of Physical Chemistry B* (Figure 3) (Zhang et al. 2006).

Citation

Zhang Z, O Bondarchuk, BD Kay, JM White, and Z Dohnalek. 2006. "Imaging Water Dissociation on TiO_2(110): Evidence for Inequivalent Geminate OH Groups." *Journal of Physical Chemistry B* 110(43): 21840-21845.

Kinetics of Microbial Reduction of Solid Phase U(VI)

C Liu,[a] Byong-Hunjeon,[b] JM Zachara,[a] Z Wang,[a] A Dohnalkova,[a] and JK Fredrickson[a]

(a) Pacific Northwest National Laboratory, Richland,Washington

(b) Yonsei University, Wonju, Kangwon-Do, Korea

Using state-of-the-art experimental techniques and geochemical modeling, the dissolution, diffusion, and microbial reduction processes of U(VI) in soils and sediments were studied. The results predicted slow U(VI) reduction in contaminated Hanford Site sediments because of high concentrations of dissolved calcium.

Microbial reduction of U(VI) by dissimilatory metal-reducing bacteria and subsequent precipitation of U(IV) has been proposed as a technology that could be used to immobilize U(VI) in uranium contaminated sediments. However, microscopic and spectroscopic analysis of uranium-contaminated sediments from the U.S. Department of Energy's Hanford Site has revealed that uranium often exists as U(VI) precipitates associated with small fractures and pores within sediment particle grains that exhibit pore sizes of a few micrometers or less. This multifacility study of microbial reduction of U(VI) solids used cryogenetic time-resolved fluorescence and geochemical modeling capabilities available in the EMSL Environmental Spectroscopy and Biogeochemistry (ESB) Facility as well as transmission electron microscope (TEM) instrumentation available in the Interfacial and Nanoscale Science Facility. The insights derived from the microscopic and spectroscopic analyses were used to establish a coupled model of dissolution, intragrain diffusion, and microbial reduction processes that lead to the ultimate formation of UO_2 precipi-tates on cell surfaces and periplasms (see Figure 1). The developed model was then applied to describe the experimental kinetic data of microbial reduction of solid phase U(VI). Of relevance to the Hanford Site, this study predicts that microbial reduction of U(VI) in contaminated sediments would proceed at two orders of magnitude slower than expected because of the high concentration of dissolved calcium in the environment (Liu et al. 2006).

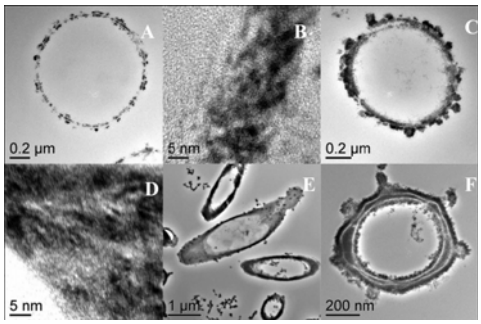

Figure 1. TEM images showing UO_2 accumulation on cell surfaces and in periplasms. Samples for images A (a sectioned cell) and B (part of a cell periplasm) were collected at 2 days, samples for images C (a sectioned cell) and D (part of a cell periplasm) were collected at 7 days, and samples for images E and F were collected at 100 days after cell spike.

Citation

C Liu, Byong-Hunjeon, JM Zachara, Z Wang, A Dohnalkova, and JK Fredrickson. 2006. "Kinetics of Microbial Reduction of Solid Phase U(VI)." *Environmental Science & Technology* 40:6290-6296.

Magnetic Resonance Imaging of Proton Exchange Membranes Dehydration and Gas Manifold Flooding During Continuous Fuel Cell Operation

KR Minard,[(a)] VV Vishwanathan,[(a)] PD Majors,[(a)] LQ Wang,[(a)] and PC Rieke[(a)]

(a) Pacific Northwest National Laboratory, Richland, Washington

The President's Hydrogen Fuel Initiative aims to reverse America's dependence on foreign oil by developing fuel cells that use hydrogen to produce electricity. Fuel cells with proton exchange membranes (PEMs) are of particular interest because they offer high power density, are lightweight and compact, operate at relatively low temperatures, and yield water as the primary byproduct of power generation.

The efficient operation of PEMs requires a delicate balance between water formation and removal because both membrane dehydration and/or flooding hinder mass transport to reactive catalytic sites. In recognition that few diagnostic tools are currently available for visualizing water distribution, EMSL users from PNNL recently described the use of magnetic resonance imaging (MRI) for this purpose (Minard et al. 2006). The work of this research team demonstrates the utility of MRI for visualizing water nonuniformity and understanding the effects on fuel cell performance. Representative images acquired over 11 hours of continuous fuel cell operation are shown in Figure 1. Briefly, they show: A, the initial water distribution within the PEM fuel cell; B and C, a dehydration front that was observed to propagate slowly over the surface of the fuel cell membrane, starting from gas inlets and progressing toward gas outlets; and C-F, the location of various flood zones within gas-delivery manifolds.

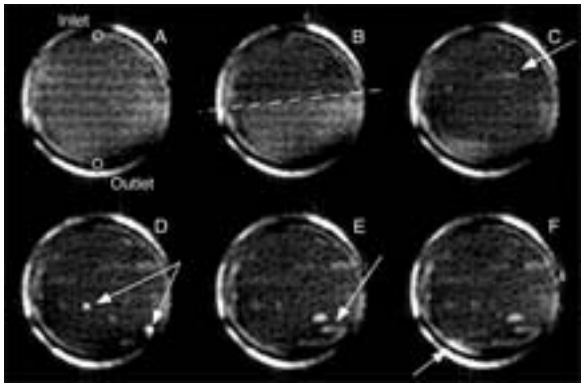

Figure 1. Selected ^{1}H water MRIs acquired at 128-second intervals over an 11-hour period. The dashed line highlights the position of the dehydration front, and the white arrows point to flooded regions.

Citation

KR Minard, VV Vishwanathan, PD Majors, LQ Wang, and PC Rieke. 2006. "Magnetic Resonance Imaging (MRI) of PEM Dehydration and Gas Manifold Flooding During Continuous Fuel Cell Operation." *Journal of Power Sources* 16(2):856-863.

Mass Spectrometry Identification of Endogenously Nitrated Proteins in Mouse Brain: Links to Neurodegenerative Disease

C A Sacksteder,[(a)] WJ Qian,[(a)] H Wang,[(a)] DJ Smith,[(b)] DJ Bigelow,[(a)] and RD Smith[(a)]

(a) Pacific Northwest National Laboratory, Richland, Washington
(b) UCLA School of Medicine, Los Angeles, California

Parkinson's, Alzheimer's, and Lou Gehrig's diseases and other brain disorders are among a growing list of maladies attributed to oxidative stress, which is the cell damage caused during metabolism when oxygen in the body assumes ever more chemically reactive forms. EMSL mass spectrometry capabilities were used to identify proteins sensitive to nitrating conditions in vivo, resulting in a dataset in which more than half the proteins were indicated in neurodegenerative disorders.

Increased nitrotyrosine modifications of proteins have been documented in multiple pathologies in a variety of tissue types linked to oxidative stress, as well as playing a role in the redox regulation of normal metabolism. To identify proteins sensitive to nitrating conditions *in vivo*, a comprehensive proteomic survey of the whole mouse brain using liquid chomatography/liquid chomatography-mass spectroscopy/mass spectroscopy (LC/LC-MS/MS) analyses was performed. This effort generated a mammalian brain dataset in which 7792 proteins were identified (Figure 1) (Sacksteder et al. 2006).

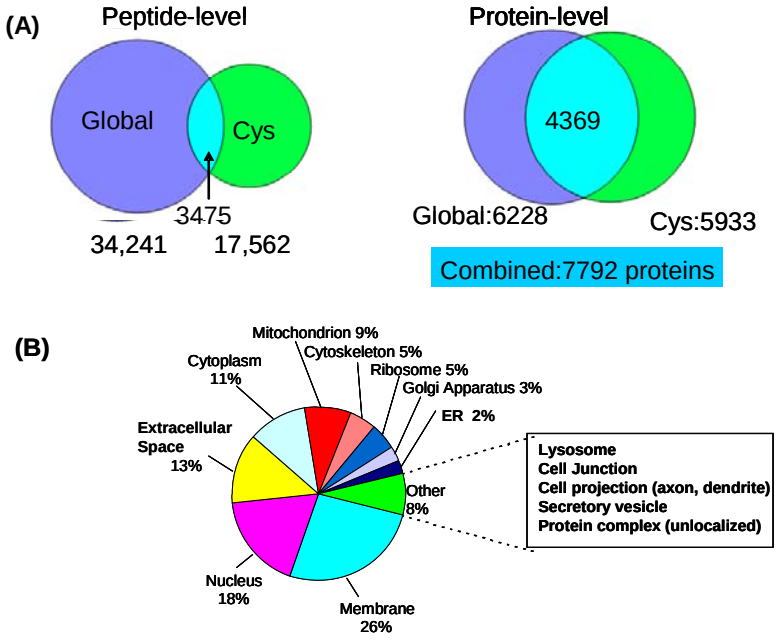

Figure 1. Extensive mouse brain proteome coverage from two-dimensional LC/LC-MS/MS analyses.

This large-scale analysis resulted in the identification of 31 unique nitrotyrosine sites within 29 different proteins. Over half of the nitrated proteins identified are involved in Parkinson's disease, Alzheimer's disease, or other neurodegenerative disorders. Similarly, nitrotyrosine immunoblots of whole-brain homogenates show that treatment of mice with 1-methyl-4-phenyl-1,2,3,6-tetrahydropyridine, an experi-mental model of Parkinson's disease, induces increased nitration of the same protein bands observed to be nitrated in brains of untreated animals. Comparing sequences and available high-resolution structures around nitrated tyrosines with those of unmodified sites indicates a preference of nitration *in vivo* for surface-accessible tyrosines in loops, a characteristic consistent with peroxynitrite-induced tyrosine modification (Figure 2). In addition, most sequences contain cysteines or methionines proximal to nitrotyrosines, contrary to suggestions that these amino acid side chains prevent tyrosine nitration. More striking is the presence of a positively charged moiety near the sites of nitration, which is not observed for non-nitrated tyrosines. Together, these observations suggest a predictive tool of functionally important sites of nitration and that cellular nitrating conditions play a role in neurodegenerative changes in the brain. Future studies should extend these proteomic

measurements to consider the relationship between protein nitration and specific neurodegenerative diseases as well as tyrosine-kinase-signaling pathways.

Citation

Sacksteder CA, WJ Qian, TV Knyushko, H Wang, MH Chin, G Lacan, WP Melega, DG Camp, RD Smith, DJ Smith, TC Squier, and DJ Bigelow. 2006. "Endogenously Nitrated Proteins in Mouse Brain: Links to Neurodegenerative Disease." *Biochemistry* 45(26):8009-8022.

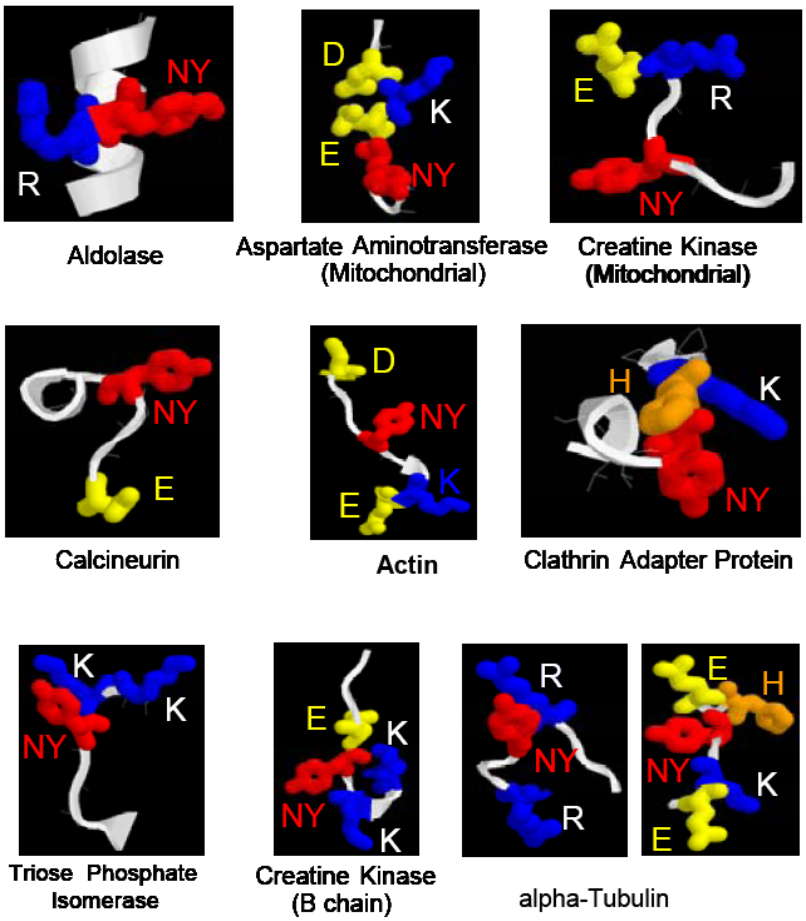

Figure 2. Three-dimensional structures around nitrotyrosines in identified proteins.

Epitaxial Growth and Microstructure of Cu_2O Nanoparticle/Thin Films on $SrTiO_3$(100)

ZQ Yu,[(a)] CM Wang,[(b)] MH Engelhard,[(b)] P Nachimuthu,[(b)] DE McCready,[(b)] IV Lyubinetsky,[(b)] and S Thevuthasan[(b)]

(a) Nanjing Normal University, Nanjing, China
(b) W.R. Wiley Environmental Molecular Sciences Laboratory, Richland, Washington

Discovering ways of using energy more efficiently and searching for new sources of energy are two major challenges for the scientific research community. Even though solar energy is recognized as a potential source of energy for human endeavors, finding a way to effectively harness this resource is still a challenge. One possible way of harnessing solar energy is to use it to separate water into its elemental components—hydrogen and oxygen—and then use the hydrogen as fuel. It has been found that cuprous oxide (CuO_2) nanoparticles may be used in this process. The goal of this research is to study the growth and morphological features of cuprous oxide nanoparticles and the optimal conditions for producing useful cuprous oxide nanoparticle.

Cu_2O is a p-type semiconductor that shows a unique electronic structure for applications related to chemical and photochemical process such as water splitting under visible light irradiation (Kosugi and Kaneko 1998; Zuo et al. 1999; Ling and Wolfe 1993; Ikeda et al. 1998; Hara et al. 1998; Lyubinetsky et al. 2003). However, Cu_2O has not been practically used for this purpose because of its low energy conversion efficiency (≤1%). Electron-hole pairs generated by light in a micron-sized Cu_2O grain are normally hard to separate. Two methods have been proposed to overcome the charge recom-bination problem. In the first method, the morphology and size of the grown Cu_2O grains is controlled, such as in the develop-ment of nanoparticles. In the second method, by choosing an appropriate substrate to grow thin film/nanoparticles of Cu_2O, a hetero-junction may be formed, which will help to effectively separate the electron-hole pairs and, therefore, to enhance the energy conversion efficiency. It has been demonstrated by Lyubinetsky et al. (2005) that molecular beam epitaxy (MBE) allows controlled growth of Cu_2O nanoparticles on a $SrTiO_3$ (STO) substrate. One of the fundamental questions that remained to be addressed is the possibility of growing stable Cu_2O thin films on an STO(100) substrate using the MBE method.

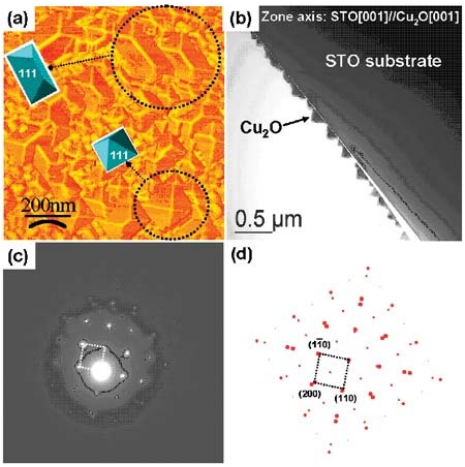

Figure 1. Microstructure of sample A. (a) atomic force microscopy (AFM) image showing the surface topographic structure of the as-deposited film. The insets are the Wulff shape construction of the Cu_2O pyramid, which is defined by the {111} planes. (b) Cross-sectional transmission electron microcopy (TEM) image showing the height of the pyramid. (c) Selected area electron diffraction pattern of both the film and the substrate, which reveals an epitaxial orientation relationship between the film and the substrate: Cu2O[001]//STO[001] and Cu2O(100)//STO(100). (d) Computer calculated diffraction pattern.

In this paper, we report the epitaxial growth of Cu_2O thin films on an STO(100) substrate. To obtain the phase of Cu_2O, the pressure-temperature phase diagram was used. The morphology of the grown Cu_2O with respect to the growth parameters, including the growth rate, was examined in detail. The films were grown in a dual-chamber ultrahigh vacuum system equipped with an electron cyclotron resonance oxygen plasma source. The details of the oxygen-plasma-assisted MBE (OPA-MBE) system along with its growth capabilities are discussed elsewhere. The *in situ* film growth was monitored using reflection high-energy electron diffraction. The chemical state of the copper at the very top of the film and inside the film was analyzed using x-ray photon-electron spectroscopy (XPS). The valence state of the copper inside the

film was analyzed following Ar^+ ion sputtering of the film to remove approximately 5 nm of top layer. The surface morphology of the as-grown layer was analyzed using atomic force microscopy (AFM). The phase of the grown layer was identified by a combination of x-ray diffraction (XRD), XPS, and cross-sectional high-resolution TEM imaging as well as selected area electron diffraction. The phase and the relative orientation of the grown film were revealed by the XRD patterns. Films grown under the two different growth rates were similarly dominated by the Cu_2O phase, which shows a preferred orientation with respect to the substrate [Cu_2O (200)//STO(100)]. A complete orientation relationship between the film and the substrate will be evaluated based on the cross-sectional TEM imaging and selected area electron diffraction as described in the subsequent sections. In addition, XRD data show the existence of trace amounts of CuO in sample A. Combined with the XPS analysis, it has been found that this minor amount of CuO phase corresponds to a surface layer of CuO on the Cu_2O (Figure 1).

Cu_2O was grown on STO(100) by OPA-MBE. The microstructure of the grown layer and the copper valence state were analyzed using XRD, XPS, AFM, and TEM as well as electron diffractions. The grown layer was dominated by the Cu_2O phase, possessing an epitaxial orientation with the substrate—Cu_2O[001]//STO[001] and Cu_2O(100)//STO(100). Cu_2O film morphologically shows dependence on the growth rate. Typically, a fast growth will lead to the formation of a thin film with a relatively smooth surface. A slow growth will lead to the development of nanoparticles, featuring the formation of Cu_2O pyramids, with the pyramids invariantly defined by the Cu_2O {111} planes. Given the fact that the {111} planes correspond to the lowest surface energy of Cu_2O, a slow growth will lend the system enough time to allow it to adopt the pyramid configuration by which the overall energy of the system was minimized.

Citations

Hara M, T Kondo, M Komoda, S Ikeda, K Shinohara, A Tanaka, JN Kondo, and K Domen. 1998. "Cu_2O as a Photocatalyst for Overall Water Splitting under Visible Light Irradiation." *Chemical Communications* 3:357-358.

Ikeda S, T Takata, T Kondo, G Hitoki, M Hara, JN Kondo, K Domen, H Hosono, H Kawazoe, and A Tanaka. 1998. "Mechano-Catalytic Overall Water Splitting." *Chemical Communications* 20:2185-2186.

Kosugi T and S Kaneko. 1998. "Novel Spray-Pyrolysis Deposition of Cuprous Oxide Thin Films." *Journal of the American Ceramic Society* 81(12):3117-3124.

Ling J and JP Wolfe. 1993. "Bose-Einstein Condensation of Paraexcitons in Stressed Cu_2O." *Physical Review Letters* 71(8):1222-1225.

Lyubinetsky I, S Thevuthasan, DE McCready, and DR Baer. 2003. "Formation of Single-Phase Oxide Nanoclusters: Cu_2O on $SrTiO_3$(100)." *Journal of Applied Physics* 94(12):7926-7928.

Lyubinetsky I, AS Lea, S Thevuthasan, and DR Baer. 2005. "Formation of Epitaxial Oxide Nanodots on Oxide Substrate: Cu_2O on $SrTiO_3$(100)." *Surface Science* 589(1-3):120-128.

Zuo JM, M Kim, M O'Keeffe, and JCH Spence. 1999. "Direct Observation of d-Orbital Holes and Cu-Cu Bonding in Cu_2O." *Nature* 401(6748):49-52.

Electron-Beam Induced Recrystallization in Amorphous Apatite

I Bae,[(a)] Y Zhang,[(b)] WJ Weber,[(a)] M Higuchi,[(c)] and LA Giannuzzi[(d)]

(a) Pacific Northwest National Laboratory, Richland, Washington
(b) W.R. Wiley Environmental Molecular Sciences Laboratory, Richland, Washington
(c) Hokkaido University, Sapporo, Japan
(d) FEI Company, Hillsboro, Oregon

Damage accumulation or recovery in certain materials under irradiation is a long lasting research topic. Crystalline apatite amorphized by energetic ion irradiation and the amorphous apatite recrystallized under further electron-beam (e-beam) irradiation are decided by local ion- and electron-solid interactions.

Apatite silicates, which are well known as extremely durable minerals, are proposed as host phases for immobilization of actinides and fission products (Weber et al. 1997). While it is known that alpha decay and heavy ion irradiation leads to amorphization of apatite materials, the effects of light ions and/or electron irradiation are not clearly understood. E-beam irradiation has proven to be capable of inducing amorphization in materials such as silicon carbide (Inui et al. 1990a; Isimaru et al. 2003), quartz (Inui et al. 1990b; Hobbs and Pascucci 1980), and coesite (Gong et al. 1996); while, in contrast, it can also cause an annealing effect in amorphous strontium titanate (Zhang et al. 2005) and other apatites (Weber and Matzke 1986; Wang and Weber 1999). Thus, the study of e-beam irradiation characteristics for apatite materials is of technological and scientific importance.

In this study, the micro-structural changes in ion-beam-amorphized $Sr_2Nd_8(SiO_4)_6O_2$ were investigated under 200 keV e-beam irradiation to further our understanding of the effects of e-beam irradiation on growth or recovery of the amorphous state. Ion irradiation, subsequent ion beam analysis based on channeling Rutherford backscattering spectroscopy (RBS), transmission electron microscope (TEM) observations, and *in situ* e-beam irradiations were performed in the EMSL.

High-dose irradiation of $Sr_2Nd_8(SiO_4)_6O_2$ by 1.0 MeV Au at 300 K leads to accumulated damage in crystal. The spectra for low-, medium-, and high-fluence irradiations illustrate the damage evolution process, where the incremental increase of the scattering yield above the virgin channeling spectrum can be easily resolved. With increasing ion fluence, the peak height increases and eventually reaches the random level. Further irradiation leads to the growth of a continuous amorphous layer that extends from the damage peak region toward the surface and into the bulk. An amorphous layer with thickness of approximately 250 nm is formed after 5.0×10^{13} cm^{-2} irradiation with some residual crystallinity at the sample surface, as shown by the lower scattering yield compared to the random yield in the inset in Figure 1.

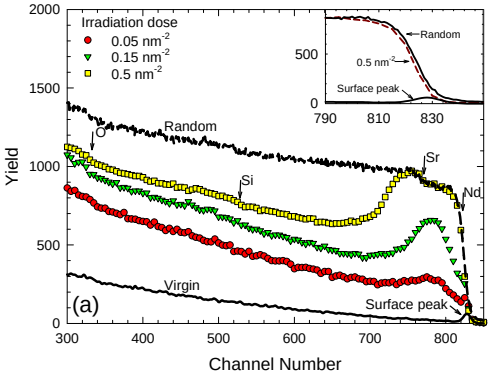

Figure 1. Series of <100>-aligned RBS spectra for $Sr_2Nd_8(SiO_4)_6O_2$ irradiated with 1.0-MeV Au^+ to different ion fluences. An enlargement of the high-energy end of the spectrum is shown as the insert.

Figure 2 shows the time evolution of e-beam-induced effects in amorphized $Sr_2Nd_8(SiO_4)_6O_2$ with an electron flux of 0.29 Å cm^{-2} (1.82 x 1018 cm^{-2s-1}) at room temperature. The initial amorphous layer before electron irradiation is shown in Figure 2(a). After 840 seconds of irradiation, recrystallization is observed from both of the amorphous/crystalline (a/c) interface and the surface. Recrystallization proceeds from both sides with almost the same rates as the electron irradiation continues to 1980 seconds. After irradiating for 3600 seconds, the recrystallization from both sides meet. It is proposed that the epitaxial recrystallization starts from

the a/c interface and the remnant crystallinity at the surface because the undamaged single crystalline substrate can act as a template material during the recrystallization process.

The recrystallization thickness is shown in Figure 3 as a function of irradiation time under two different electron fluxes. For both electron fluxes, the recrystallization process shows two linear stages: rapid regrowth up to approximately 250 seconds followed by a slower regrowth that is strongly flux-dependent up to measurement times of approximately 3000 seconds. The rapid motion of the a/c interface during the initial stage is considered to be associated with electron-enhanced defect annihilation at a/c interface, similar to that observed in $SrTiO_3$. Besides, nanocrystallities, which are considered to exist at the a/c interface, are also considered to play a role for the rapid motion of the a/c interface. After the initial stages, at which most of the defects near the a/c interface have been annihilated, the recrystallization processes are stabilized at decreasing rates as indicated by the decreased slopes with further irradiation time.

Ionization-induced processes, in which incident electrons primarily transfer their energy by inelastic interaction with target atoms to induce localized electronic excitations, may play an important role for the observed recrystallization in this work. Since the localized electronic excitations can disturb local atomic bonds and structure, they may effectively lower the energy barrier for defect recovery and recrystallization processes, which may involve local atomic hopping or rotation of atomic polyhedra (Zhang et al. 2005).

In conclusion, epitaxial recrystallization is observed from both the amorphous/crystalline interface and the surface, and the recrystallization is more pronounced with increasing e-beam flux. Because the temperature increase induced by e-beam irradiation is estimated to be less than 7 K and maximum energies transferred to target atoms are below the displacement energies, ionization-induced processes are considered to be the primary mechanisms for the solid-phase epitaxial recrystallization observed in this study.

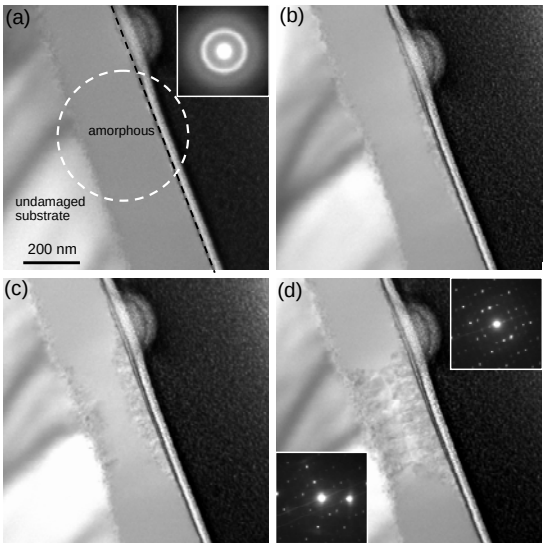

Figure 2. Structural changes of $Sr_2Nd_8(SiO_4)_6O_2$ under electron irradiation: (a) 0 seconds, (b) 840 seconds, (c) 1980 seconds, (d) 3600 seconds. Electron flux was fixed at 0.29 A cm-2 (1.82 x 1018 cm-2s-1).

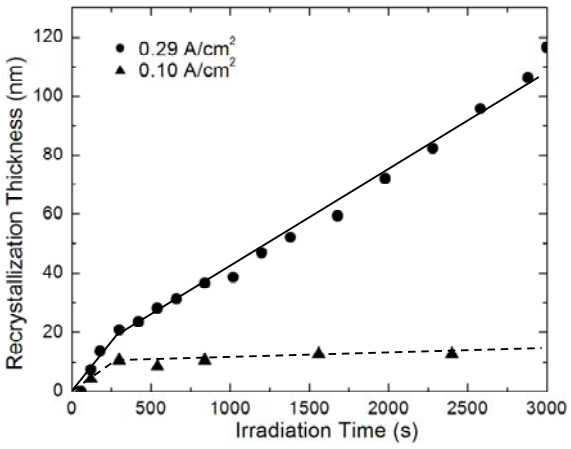

Figure 3. Amorphous-to-crystalline phase transition as a function of 200-keV e-beam irradiation time under two different electron fluxes at RT.

Citations

Gong WL, LM Wang, RC Ewing, and J Zhang. 1996. "Electron-Irradiation- and Ion-Beam-Induced Amorphization of Cosite." *Physical Review B* 54(6):38003808.

Hobbs LW and MR Pascucci. 1980. "Radiolysis and Defect Structure in Electron-Irradiated α-Quartz." *Journal de Physique Colloque* 41(C6):237-242.

Inui H, H Mori, and H Fujita. 1990a. "Electron-Irradiation-Induced Crystalline to Amorphous Transition in Alpha-SiC Single Crystals." *Philosophical Magazine B* 61(1):107-124.

Inui H, H Mori, T Sakata, and H Fujita. 1990b. "Electron-Irradiation-Induced Crystalline-to-Amorphous Transition in Quartz Single Crystals." *Journal of Non-Crystalline Solids* 116(1):1-15.

Ishimaru M, IT Bae, and Y Hirotsu. 2003. "Electron-Beam-Induced Amorphization in SiC." *Physical Review B* 68(14): Article No. 144102.

Wang LM, and WJ Weber. 1999. "Transmission Electron Microscopy Study of Ion-Beam-Induced Amorphization of $Ca_2La_8(SiO_4)_6O_2$." *Philosophical Magazine A* 79(1):237-253.

Weber WJ and H Matzke. 1986. "Effects of Radiation on Microstructure and Fracture and Fracture Properties in $Ca_2Nd_8(SiO_4)_6O_2$." *Materials Letters* 5(1-2):9-16.

Weber WR, RC Ewing, and A Meldrum. 1997. "The Kinetics of Alpha-Decay-Induced Amorphization in Zircon and Apatite Containing Weapons-Grade Plutonium or Other Actinides." *Journal of Nuclear Materials* 250(2-3)147-155.

Zhang Y, J Lian, CM Wang, W Jiang, RC Ewing, and WJ Weber. 2005. "Ion-Induced Damage Accumulation and Electron-Beam-Enhanced Recrystallization in $SrTiO_3$." *Physical Review B* 72(9):Article No. 094112.

A Quantitative Account of Quantum Effects in Liquid Water

GS Fanourgakis,[(a)] GK Schenter,[(a)] and SS Xantheas[(a)]

(a) Pacific Northwest National Laboratory, Richland, Washington

Since the first electrostatic interaction potential introduced by Bernal and Fowler in 1933 and the first computer simulations for its liquid state by Baker and Stillinger in 1969 and Rahman and Stillinger in 1971, water still remains an active field of research.

A comprehensive model describing water and its anomalous properties has yet to be developed. Most existing potentials for water have been parametrized to reproduce its macroscopic structural and thermodynamic properties using classical molecular dynamics simulations. These models are, however, appropriate for classical molecular dynamics simulations only for the particular phase that was included in the training set. Truly "transferable" models require an accurate representation of underlying Born-Oppenheimer potential energy surface and explicit account of zero-point-energy effects.

An alternative to classical potentials is evaluation of the electronic energy and forces from first principles. The authors report converged quantum statistical mechanical simulations of liquid water with the Thole model, flexible, polarizable (TTM2.1-F) interaction potential for water. The quantum statistical mechanical radial distribution functions (RDFs) and average energy of the system were sampled using centroid molecular dynamics. Simulations with a total duration of 600 ps with 0.05-fs time steps for a periodic unit cell of 256 molecules with up to 32 replicas per atom suggest that the quantum effects contribute 1.01 ±0.02 kcal/mol to the liquid enthalpy of formation at 298.15 K. They furthermore demonstrate a first-time quantitative agreement with experimental results for the heights and broadening of the intramolecular OH and HH peaks in the radial distribution functions (see Figure 1). The results presented in this paper clearly identify a path for obtaining accurate structural and thermodynamic information of complex, many-body systems, and lay the foundation for forthcoming studies of other thermodynamic states of water and the examination of its anomalous properties (Fanourgakis et al. 2006; Thole 1981; Kuharski and Rossky 1985).

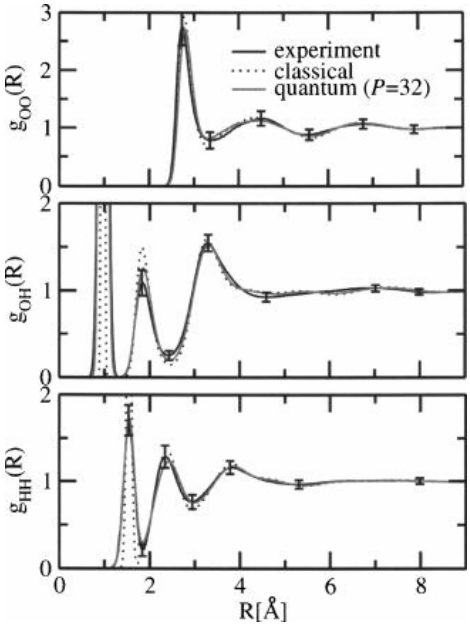

Figure 1. Calculated quantum statistical mechanical and experi-mental RDFs for oxygen-oxygen, oxygen-hydrogen, and hydrogen-hydrogen at T=298.15 K. The error bars correspond to the experimental uncertainty.

Citations

Fanourgakis GS, GK Schenter, and SS Xantheas. 2006. "A Quantitative Account of Quantum Effects in Liquid Water." *Journal of Chemical Physics* 125(14): Article No. 141102.

Kuharski RA and PJ Rossky. 1985. "A Quantum-Mechanical Study of Structure in Liquid H_2O and D_2O." *Journal of Chemical Physics* 82(11):5164.

Thole BT. 1981. "Molecular Polarizabilities Calculated with a Modified Dipole Interaction." *Chemical Physics* 59(3):341-350.

Asymptotic Extrapolation Scheme for Large-Scale Calculations with Hybrid Coupled-Cluster and Molecular Dynamics Simulations

K Kowalsk[(a)] and M Valiev[(a)]

(a) W.R. Wiley Environmental Molecular Sciences Laboratory, Richland, Washington

While high-level coupled cluster (CC) calculations currently are possible for small- and medium-size molecular systems, the development of accurate, excited-state methods for larger, biologically relevant systems pose a significant challenge for theory.

Usually, the size of biologically important systems prohibits the use of highly correlated *ab initio* methods and extensive basis sets that include diffuse functions or functions of triple- or quadruple-ζ quality. On the other hand, these factors are imperative in understanding photophysical and photochemical properties of nucleic acids, especially those related to the ultraviolet (UV)-protection mechanism based on the ultrafast conversion of excited electronic states. Recently, the authors developed, using NWChem capabilities, a suite of programs that combines classical molecular dynamics with high-level *ab initio* methods for excited states (Kowalski and Valiev 2006). The main goal of this effort was to create a framework for realistic, temperature-dependent, excited-state calculations for biochemical systems with an approximate description of the effects of the native environment, including its dynamical fluctuations. Because thermal averaging involves multiple calls to rather expensive *ab initio* procedures, the low-scaling extrapolation schemes may play a pivotal role in further advancing this area. The main purpose of this paper is to address, on a very basic level, these important issues. A very simple τ-parameter dependent cut-off scheme was used for the virtual orbitals, with orbital energies lying above the cut-off factor. Based on this scheme, simple heuristic formulas were derived for the excitation energies as a function of the τ-parameter, subsequently used in the extrapolation procedures that describe an asymptotic dependence of τ-dependent energies. The performance of the asymptotic extrapolation scheme for completely re-normalized equation-of-motion approach with singles, doubles, and noniterative triples (CR-EOMCCSD(T)) methods is illustrated on the excited-state calculation of cytosine (see Figure 1) base in its native DNA environment. We have clearly shown that:

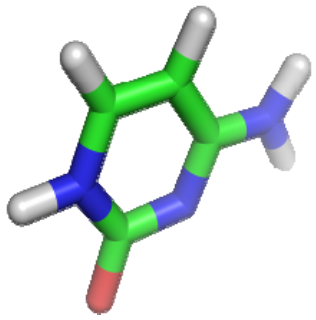

Figure 1. The structure of excited states of the cytosine molecule plays an important role in understanding photo-stability of DNA.

1. Errors resulting from the extrapolation procedure are negligible when compared to standard fluctuations in the excitation-energy values caused by a fluctuating environment.

2. Use of the asymptotic extrapolation scheme results in more than two orders of magnitude speedups of the CR-EOMCCSD(T) codes with insignificant loss of accuracy on the order of few hundreds of electron volts. Further development of the asymptotic extrapolation scheme in the context of high-level *ab initio* methodologies should lead to the routine use of the highly correlated methods in studies of photoinduced processes in biologically relevant systems.

Citation

Kowalski K and M Valiev. 2006. "Asymptotic Extrapolation Scheme for Large-Scale Calculations with Hybrid Coupled Cluster and Molecular Dynamics Simulations." *Journal of Physical Chemistry A*, 110(48): 13106-13111.

Scientific Grand Challenge Highlights

Characterization of Two Potentially Universal Turn Motifs that Shape the Repeated Five-Residue Fold-Crystal Structure of a Lumenal Pentapeptide Repeat Protein from *Cyanothece* 51142

GW Buchko,[(a)] S Ni,[(a)] H Robinson,[(b)] EA Welsh,[(c)] HB Pakrasi,[(c)] and MA Kennedy[(a)]

(a) Pacific Northwest National Laboratory, Richland, Washington
(b) Brookhaven National Laboratory, Upton, New York
(c) Washington University, St. Louis, Missouri

The crystal structure was determined for Rfr32, which is one of 35 pentapeptide repeat proteins (PRPs) in the diurnal cyanobacterium Cyanothece. The structure is dominated by 21 tandem pentapeptide repeats that fold into a right-handed quadrilateral ß-helix, or Rfr-fold. Analysis of the main chain (Φ, Ψ) dihedral orientations for the pentapeptide repeats reveals structural details for the two distinct types of four-residue turns adopted by the pentapeptide repeats in the Rfr-fold, labeled type-II and type-IV ß-turns, that may be universal motifs that shape the Rfr-fold in all PRPs.

HB Pakrasi and his colleagues at Washington University (WU) in St. Louis, Missouri, have recently sequenced the genome of the diurnal cyanobacterium *Cyanothece* sp. PCC 51142. One of the interesting features of the genome, as determined by the annotation team led by WU's E Welsh, is the presence of 35 proteins containing tandem pentapeptide repeats. Such PRPs are identified by the presence of at least eight consecutive repeating five-residues (RFR) approximately described by the consensus motif A[D/N]LXX. While such proteins are scattered throughout the genomes of organisms in both the prokaryotic and eukaryotic kingdoms, PRPs are especially abundant in cyanobacteria. The sheer number of PRPs in cyanobacteria coupled with their predicted location in every cellular compartment argues for an important, yet unknown, physiological and biochemical function. To gain biochemical insights into this mystery, we have determined the crystal structure for one of the 35 PRP in *Cyanothece*, Rfr32, as part of an EMSL Molecular Biology Scientific Grand Challenge project.

Rfr32 is a 167-residue PRP with an N-terminal, 29-residue signal peptide. As shown in Figure 1, the protein construct of Rfr32 lacking the 29-residue signal peptide crystallized in two different forms that yielded identical structures. H Robinson at Brookhaven National Laboratory collected x-ray data at the National Synchrotron Light Source on these crystals that diffracted to a resolution of 2.1 Å. Figures 2A and B are graphical representations of the structure.

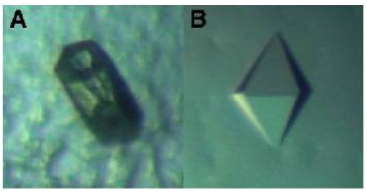

Figure 1. Two different crystal forms of Rfr32 grown using the hanging-drop, vapor-diffusion method at 6x magnification: A, hollow rods with a hexagonal face and B, bipyrimides.

The dominant feature is the novel type of right-handed quadrilateral ß-helix, a repeated five-residue fold (Rfr-fold), adopted by the 21 consecutive pentapeptide repeats. This Rfr-fold is reminiscent of a square tower with four distinct faces with each pentapeptide repeat occupying one face of the Rfr-fold. Four consecutive pentapeptide repeats complete a coil that makes a revolution with approximately a 4.8-Å increase every 20 residues. A stylized representation of a complete coil in an Rfr-fold, which is the higher-order structural unit adopted by four tandem pentapeptide repeats, is shown in Figure 2C. The coils of the tower in Rfr32 are held together by short stretches of parallel ß-sheets (Face 1) and ß-bridges (Faces 2-4) (single-residue ß-sheets), which are integral to the quadrilateral shape of the Rfr-fold. There is a regular orientation of the side chains of each pentapeptide repeat. Designating the center residue of each pentapeptide repeat i with the preceding residues labeled i-1 and i-2 and the following residues labeled i+1 and i+2, we observed that the i-2 and I residues all point toward the interior of the tower

and pack the middle of the Rfr-fold. The side chain of the ith residue is predominately a large hydrophobic group (Leu or Phe), while the side chain of the i-2 residue is predominately a small and usually hydrophobic group (Ala > Ser, Thr, and Val). On the other hand, the side chains of the i-1, i+1, and i+2 residues all point away from the interior of the tower and form the exterior, solvent-exposed surface of the Rfr-fold. Unlike the side chains that are directed to the interior, which are primarily hydrophobic and form regularly stacked columns, the side chains directed to the exterior are typically hydrophilic and do not assume a regular form.

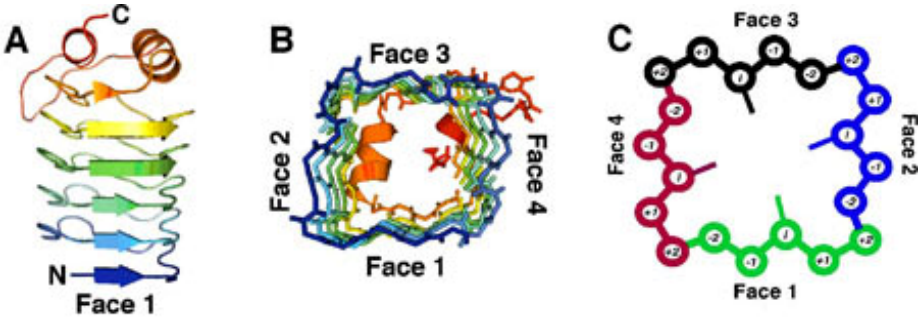

Figure 2. Graphical representations of the Rfr32 (PDB ID - 2F3L) crystal structure: A, side-view; B, top-view of A viewed from the C-terminal; and C, stylized representation of a complete coil in an Rfr-fold, the higher-order structural unit adopted by four tandem pentapeptide repeats. Each pentapeptide repeat is colored differently and is labeled relative to the central residue *i*.

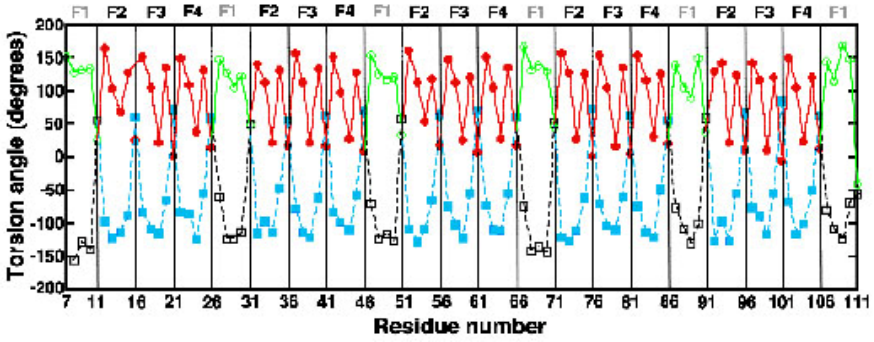

Figure 3. Plot of the main chain (Φ,Ψ) dihedral torsion angles for the 21 consecutive pentapeptide repeats (A7-V111) that make up the Rfr-fold of Rfr32. The Φ torsion angles are connected with a dashed line and labeled with open black squares for the residues in Face 1 and closed blue squares for residues in Faces 2-4. The Ψ torsion angles are connected with a solid line and labeled with open green circles for residues in Face 1 and closed red circles for residues in Faces 2-4.

Figure 3 is a plot of the main chain (Φ, Ψ) dihedral orientations for Rfr32 residues A7-V111 that make up the Rfr-fold. Clearly, two distinct patterns are observed for the five residues constituting each coil on Face 1 and for the five residues constituting each coil on Faces 2, 3, and 4. After thorough analysis of the crystal structures of Rfr32 and MfpA (from *Mycobacterium tuberculosis*), it became evident that each pentapeptide repeat could be grouped into one of two types of four-residue type II and type IV ß-turns. The major differences between the two types of ß-turns is the Ψ and Φ torsion angles of the i and i+1 residue results from an ~90° rotation of the peptide unit between these two residues. Because of the repetitive nature of the pentapeptide repeat sequence, we predict that the regular shape of the Rfr-fold is maintained by these two distinct ß -turns and that they may be universal motifs that shape the Rfr-fold in all pentapeptide repeat proteins. The results of this Scientific Grand Challenge project were published in the journal *Protein Science* (Buchko et al. 2006)

Citation

Buchko GW, S Ni, H Robinson, EA Welsh, HB Pakrasi, and MA Kennedy. 2006. "Characterization of Two Potentially Universal Turn Motifs that Shape the Repeated Five-Residue Fold-Crystal Structure of a Lumenal Pentapeptide Repeat Protein from *Cyanothece* 51142." *Protein Science* 15(11):2579-2595.

Awards and Recognition

EMSL user J Laskin was co-editor of the new book *Principles of Mass Spectrometry Applied to Biomolecules*. The book has 16 chapters written by experts in the field of fundamental mass spectrometry and gas-phase ion chemistry. Laskin of PNNL and LS Wang of Washington State University Tri-Cities wrote two of the chapters. Another chapter written by EMSL user G Cooks of Purdue University provides information on the EMSL Science Theme proposal he leads.

Professional/Community Service

In mid-November, EMSL staff members KM Regimbal, T Carlson, EJ Felix, and R Farber attended SuperComputing 2006 (SC06), which is the annual conference held to share research and accomplishments, learn about and debate the latest issues and best practices, and interact with the best minds in high-performance computing. Carlson led a team of PNNL scientists who were finalists in the SC06 Bandwidth Challenge. The feature application of the PNNL team was Polygraph, a high-performance implementation of a statistical and physical model-based, feature-matching algorithm written by CS Oehmen and DJ Baxter. Polygraph was run on a Beowulf cluster located on the SC06 show floor communicating with a Lustre file system located in PNNL's Secure Collaboration Zone. While the PNNL team did not achieve the through-put it had hoped for, the team learned many valuable lessons concerning the deployment of Lustre in a Wide Area Network setting.

Carlson, Baxter, and ER Vorpagel also were members of PNNL's Analytics Challenge entry at SC06. The PNNL entry was nominated as one of three finalists. The Analytics Challenge showcased the Bioinformatics Resource Manager, which enables scientists to go from experimental spectra to pathway data in a single workflow, thereby reducing the time-to-solution for analyzing biological data from weeks to minutes.

Major Facility Upgrades

Gas purification systems used on the four anaerobic environmental glove boxes in the ESB Facility were recently replaced by enhanced two-column gas purification systems. The new dual-column system will allow the low oxygen/moisture atmosphere to be maintained while regenerating the purification system by switching between the two catalyst columns. This eliminated the need to take the chamber out of use and the attendant exposure of samples to high-oxygen conditions for at least 24 hours while the catalyst is regenerated. The new systems are controlled by a user-friendly touch screen.

News Coverage

In the October 4, 2006, edition of *Science Daily*, work performed by a PNNL team headed by L Shi was featured in an article entitled "Slippery Salmonella: Proteomics Exposes an Infectious Agent of Deception." The full article can be viewed at http://www.sciencedaily.com/releases/2006/09/060929093337.htm.

Visitors and Users

During this reporting period (October through November 2006), a total of 323 users benefited from EMSL capabilities and the expertise of EMSL staff members. This total included 180 onsite users and 143 remote users.

New EMSL Staff

DML Brown, formerly a Science and Engineering Education Intern at PNNL, joined MSCF Operations in November. Brown has experience working with Linux Kernal Programing, system administration, and source code management.

A Liyu joined the Instrument Development Laboratory in October.

Publications

Alexandrova AN, AI Boldyrev, HJ Zhai, and LS Wang. 2006. "All-Boron Aromatic Clusters as Potential New Inorganic Ligands and Building Blocks in Chemistry." *Coordination Chemistry Reviews* 250(21-22):2811-2866.

Anderson JA, BW Hoplins, and J Chapman. 2006. "A Systematic Assessment of Density Functionals and ONIOM Schemes for the Study of Hydrogen Bonding Between Water and the Side Chains of Serine, Threonine, Asparagine, and Glutamine." *Journal of Molecular Structure - Theochem* 771(1-3):65-71.

Antony J, S Pendyala, DE McCready, MH Engelhard, D Meyer, A Sharma, and Y Qiang. 2006. "Ferromagnetism in Ti-Doped ZnO Nanoclusters above Room Temperature." *IEEE Transactions on Magnetics* 42(10):2697-2699. doi:10.1109/TMAG.2006.879723

Averkiev BB, AI Boldyrev, X Li, and LS Wang. 2006. "Planar Nitrogen-Doped Aluminum Clusters Al_xN^- (x=3-5)." *Journal of Chemical Physics* 125(12): Art. No. 124305 (12 pages).

Baas T, CR Baskin, DL Diamond, A Garcia-Sastre, H Bielefeldt-Ohmann, TM Tumpey, MJ Thomas, VS Carter, TH Teal, N Van Hoven, S Proll, JM Jacobs, Z Caldwell, MA Gritsenko, R Hukkanen, DG Camp II, RD Smith, and MG Katze. 2006. "Integrated Molecular Signature of Disease: Analysis of Influenza Virus-Infected Macaques through Functional Genomics and Proteomics." *Journal of Virology* 80(21):10813-10828. doi:10.1128/JVI.00851-06

Barcaro G, A Fortunelli, G Rossi, F Nita, and R Ferrando. 2006. "Electronic and Structural Shell Closure in AgCu and AuCu Nanoclusters." *Journal of Physical Chemistry B* 110(43):23197-23203.

Bertino MF, Z Sun, R Zhang, and LS Wang. 2006. "Facile Syntheses of Monodisperse Ultra-Small Au Clusters." *Journal of Physical Chemistry B* 110(43):21416-21418. doi:10.1021/jp065227g

Buchko GW, S Ni, H Robinson, EA Welsh, HB Pakrasi, and MA Kennedy. 2006. "Characterization of Two Potentially Universal Turn Motifs that Shape the Repeated Five-Residues Fold - Crystal Structure of a Lumenal Pentapeptide Repeat Protein from *Cyanothece* 51142." *Protein Science* 15(11):2579-2595.

Cermelli S, Y Guo, SP Gross, and M Welte. 2006. "The Lipid-Droplet Proteome Reveals that Droplets Are a Protein-Storage Depot." *Current Biology* 16(18):1783-1795. doi:10.1016/j.cub.2006.07.062

Cheng C, JS Evans, and VT Voorhis. 2006. "Simulating Molecular Conductance Using Real-Time Density Functional Theory." *Physical Review B. Condensed Matter and Materials Physics* 74(15):155112.

Dantas G, AL Watters, B Lunde, Z Eletr, NG Isern, J Lipfert, S Doniach, B Kuhlman, BL Stoddard, G Varani, and D Baker. 2005. "Mis-translation of a Computationally Designed Protein Yields an Exceptionally Stable Symmetric Homodimer: Implications for Protein Engineering and Evolution." *Journal of Molecular Biology* 362(5):1004-1024.

Dobson N, G Dantas, DA Baker, and G Varani. 2006. "High-Resolution Structural Validation of the Computational Redesign of Human U1A." *Structure* 14(5):847-856.

Dohnalek Z, J Kim, and BD Kay. 2006. "Growth of Epitaxial Thin Pd(111) Films on Pt(111) and Oxygen-Terminated FeO(111) Surfaces." *Surface Science* 600(17):3461-3471.

Eslinger PW, CT Kincaid, WE Nichols, and SK Wurstner. 2006. "A Demonstration of the System Assessment Capability (SAC) Rev. 1 Software for the Hanford Remediation Assessment Project." PNNL-16209, Pacific Northwest National Laboratory, Richland, Washington.

Fanourgakis GS, GK Schenter, and SS Xantheas. 2006. "A Quantitative Account of Quantum Effects in Liquid Water." *Journal of Chemical Physics* 125(14): Art. No. 141102.

Farnan I, HM Cho, and WJ Weber. 2006. "Identifying and Quantifying Actinide Radiation Damage in ZrSiO4 Minerals and Ceramics with Nuclear Magnetic Resonance." In *Proceedings of the Eighth Actinides Conference*, *Actinides 2005*, 4-8 July 2005, University of Manchester, United Kingdom. Published in *Recent Advances in Actinide Science*, eds. R Alvarez, N Bryan, I May, pp. 305-310. Royal Society of Chemistry, Cambridge, United Kingdom.

Gibbs GV, D Jayatilaka, MA Spackman, DF Cox, and KM Rosso. 2006. "Si-O Bonded Interactions in Silicate Crystals and Molecules: A Comparison." *Journal of Physical Chemistry A* 110(46): Art. No. 12678-12683.

Gibbs GV, MA Spackman, D Jayatilaka, KM Rosso, and DF Cox. 2006. "Bond Length and Local Energy Density Property Connections for Non-transition-Metal Oxide-Bonded Interactions. " *Journal of Physical Chemistry A* 110(44):12259-12266.

Gutowski KE and DA Dixon. 2006. "*Ab Initio* Prediction of the Gas- and Solution-Phase Acidities of Strong Bronsted Acids: The Calculation of pK(a) Values Less than -10." *Journal of Physical Chemistry A* 110(43):12044-12054.

Gutowski KE, RD Rogers, and DA Dixon. 2006. "Accurate Thermochemical Properties for Energetic Materials Applications. I. Heats of Formation of Nitrogen-Containing Heterocycles and Energetic Precursor Molecules from Electronic Structure Theory." *Journal of Physical Chemistry A* 110(42):11890-11897.

Herzog E, T Frigato, V Helms, and CD Lancaster 2006. "Energy Barriers of Proton Transfer Reactions between Amino Acid Side Chain Analogs and Water from *ab initio* Calculations." *Journal of Computational Chemistry* 27(13):1534-1547.

Hixson KK, JN Adkins, SE Baker, RJ Moore, RD Smith, SL McCutchen-Maloney, and MS Lipton. 2006. "Biomarker Candidate Identification in *Yersinia pestis* Using Organism-Wide Semiquantitative Proteomics." *Journal of Proteome Research* 5(11):3008-3017.

Johnson KS, B de Foy, BM Zuberi, L Molina, MJ Molina, Y Xie, A Laskin, and V Shutthanandan. 2006. "Aerosol Composition and Source Apportionment in the Mexico City Metropolitan Area with PIXE/PESA/STIM and Multivariate Analysis." *Atmospheric Chemistry and Physics* 6(12):4591-4600.

Johnson TJ, SW Sharpe, and MA Covert. 2006. "Disseminator for Rapid, Selectable, and Quantitative Delivery of Low and Semivolatile Liquid Species to the Vapor Phase." *Review of Scientific Instruments* 77(9): Art. No. 094103 (7 pages).

Joly AG, M Henyk, KM Beck, PE Trevisanutto, PV Sushko, WP Hess, and AL Shluger. 2006. "Probing Electron Transfer Dynamics at MgO Surfaces by Mg-Atom Desorption." *Journal of Physical Chemistry B* 110(37):18093-18096.

Kelly RT, JS Page, Q Luo, RJ Moore, DJ Orton, K Tang, and RD Smith. 2006. "Chemically Etched Open Tubular and Monolithic Emitters for Nanoelectrospray Ionization Mass Spectrometry." *Analytical Chemistry* 78(22):7796-7801.

Kiran B, X Li, HJ Zhai, and LS Wang. 2006. "Gold as Hydrogen: Structural and Electronic Properties and Chemical Bonding in $Si_3Au3^{+/0/-}$ and Comparisons to $Si_3H3^{+/0/-}$." *Journal of Chemical Physics* 125(13): Art. No. 133204 (7 pages).

Kowalski K and M Valiev. 2006. "Asymptotic Extrapolation Scheme for Large-Scale Calculations with Hybrid Coupled Cluster and Molecular Dynamic Simulations." *Journal of Chemical Physics* 110(48):13106-13111.

Kwak J, D Kim, T Szailer, CH Peden, and J Szanyi. 2006. "NOx Uptake Mechanism on Pt/BaO/Al2O3 Catalysts." *Catalysis Letters* 111(3-4):119-126.

Ling S, W Yu, Z Huang, Z Lin, M Haranczyk, and MS Gutowski. 2006. "Gaseous Arginine Conformers and Their Unique Intramolecular Interactions." *Journal of Physical Chemistry A* 110(44):12282-12291.

Lins Neto RD and R Ferreira. 2006. "The Stability of Right- and Left-Handed Alpha-Helices as a Function of Monomer Chirality." *Quimica Nova* 29(5):997-998.

Liu C, B Jeon, JM Zachara, Z Wang, A Dohnalkova, and JK Fredrickson. 2006. "Kinetics of Microbial Reduction of Solid Phase U(VI)." *Environmental Science & Technology* 40(20):6290-6296.

Liu G, J Wang, H Wu, and Y Lin. 2006. "Versatile Apoferritin Nanoparticle Labels for Assay of Protein." *Analytical Chemistry* 78(21):7417-7423. doi:10.1021/ac060653j

Liu L, MH Engelhard, and M Yan. 2006. "Surface and Interface Control on Photochemically Initiated Immobilization." *Journal of the American Chemical Society* 128(43):14067-14072.

Liu T, W Qian, MA Gritsenko, W Xiao, LL Moldawer, A Kaushal, ME Monroe, SM Varnum, RJ Moore, SO Purvine, RV Maier, RW Davis, RG Tompkins, DG Camp II, and RD Smith. 2006. "High Dynamic Range Characterization of the Trauma Patient Plasma Proteome." *Molecular & Cellular Proteomics* 5(10): 1899-1913.

Lumetta GJ, RS Addleman, BP Hay, TL Hubler, TG Levitskaia, SI Sinkov, LA Snow, MG Warner, and SL Latesky. 2006. *Selective Media for Actinide Collection and Pre-Concentration: Results of FY 2006 Studies.* PNNL-16213, Pacific Northwest National Laboratory, Richland, Washington.

Manna S, E Zangrando, A Bencini, C Benelli, and N Chaudhuri. 2006. "Syntheses, Crystal Structures, and Magnetic Properties of [Ln(III)2(succinate) (3)(H²O)(2)]Center Dot 0.5H(2)O [Ln = Pr, Nd, Sm, Eu, Gd, and Dy] Polymeric Networks: Unusual Ferromagnetic Coupling in Gd Derivative." *Inorganic Chemistry* 45(22):9114-9122.

Minard KR, VV Vishwanathan, PD Majors, LQ Wang, and PC Rieke. 2006. "Magnetic Resonance Imaging (MRI) of PEM Dehydration and Gas Manifold Flooding During Continuous Fuel Cell Operation." *Journal of Power Sources* 161(2):856-863.

Naumkin FY. 2006. "Metastable Intermolecular Charge-Transfer Complexes with a Pentavalent Carbon Atom." *Journal of Physical Chemistry* 110(40):11392-11395.

Oostrom M, C Hofstee, and TW Wietsma. 2006. "Behavior of a Viscous LNAPL under Variable Water Table Conditions." *Soil & Sediment Contamination* 15(6):543-564.

Petrik NG, AG Kavetsky, and GA Kimmel. 2006. "Electron-Stimulated Production of Molecular Oxygen in Amorphous Solid Water on Pt(111): Precursor Transport through the Hydrogen Bonding Network." *Journal of Chemical Physics* 125(12): Art. No. 124702 (11 pages).

Qian WJ; JM Jacobs, T Liu, DG Camp II, and RD Smith. 2006. "Advances and Challenges in Liquid Chromatography-Mass Spectrometry-Based Proteomics Profiling for Clinical Applications." *Molecular & Cellular Proteomics* 5(10):1727-1744.

Ramirez JZ, R Vargas, J Garza, and BP Hay. 2006. "Performance of the Effective Core Potentials of Ca, Hg, and Pb in Complexes with Ligands Containing N and O Donor Atoms." *Journal of Chemical Theory and Computation* 2(6)L1510-1519

Rodriguez LG, SJ Lockett, and GR Holtom. 2006. "Coherent Anti-Stokes Raman Scattering Microscopy: A Biological Review." *Cytometry Part A* 69A(8):779-791.

Shvartsburg AA, T Bryskiewicz, R Purves, K Tang, R Guevremont, and RD Smith. 2006. "Field Asymmetric Waveform Ion Mobility Spectrometry Studies of Proteins: Dipole Alignment in Ion Mobility Spectrometry?" *Journal of Physical Chemistry B* 110(43):21966-21980. doi:10.1021/jp062573p

Sioutis I and RM Pitzer. 2006. "Theoretical Investigation of the Binding Energies of the Iodide Ion and Xenon Atom with Decaborane." *Journal of Physical Chemistry A* 110:12528-12537.

Van Dam H, MF Guest, P Sherwood, J Thomas, J Van Lingen, C Bailey, and I Bush. 2006. "Large-Scale Electronic Structure Calculations in the Study of the Condensed Phase." *Journal of Molecular Structure - Theochem* 771(1-3):33-41.

Wang J, G Liu, MH Engelhard, and Y Lin. 2006. "Sensitive Immunoassay of a Biomarker Tumor Necrosis Factor-[alpha] Based on Poly(guanine)-Functionalized Silica Nanoparticle Label." *Analytical Chemistry* 78(19):6974-6979. doi:10.1021/ac060809f

Wang XB, YL Wang, HK Woo, J Li, GS Wu, and LS Wang. 2006. "Free Tetra- and Hexa-Coordinated Platinum-Cyanide Dianions, $Pt(CN)^{2-}_4$ and $Pt(CN)^{2-}_6$: A Combined Photodetachment Photoelectron Spectroscopic and Theoretical Study." *Chemical Physics* 329(1-3):230-238.

Wang XB, HK Woo, B Jagoda-Cwiklik, P Jungwirth, and LS Wang. 2006. "First Steps towards Dissolution of $NaSO_4^-$ by Water." *Physical Chemistry Chemical Physics* 8(37):4294-4296.

Waters T, X Huang, XB Wang, HK Woo, RAJ O'Hair, AG Wedd, and LS Wang. 2006. "Photoelectron Spectroscopy of Free Multiply Charged Keggin Anions α-$[PM_{12}O_{40}]^{3-}$ (M = Mo, W) in the Gas Phase." *Journal of Physical Chemistry A* 110(37):10737-10741.

Woo HK, KC Lau, XB Wang, and LS Wang. 2006. "Observation of Cysteine Thiolate and S-Center Dot Center Dot Center Dot H-O Intermolecular Hydrogen Bond." *Journal of Physical Chemistry A* 110(46): 12603-12606.

Wu Q and T Van Voorhis. 2006. "Extracting Electron Transfer Coupling Elements from Constrained Density Functional Theory." *Journal of Chemical Physics* 125(16):164105.

Yantasee W, GE Fryxell, and Y Lin. 2006. "Voltammetric Analysis of Europium at Screen-Printed Electrodes Modified with Salicylamide Self-Assembled on Mesoporous Silica." *Analyst* 131(12):1342-1346. doi:10.1039/b609211j

Zhai HJ and LS Wang. 2006. "Probing the Electronic Properties of Dichromium Oxide Clusters $Cr_2O_n^-$ (n=1-7) Using Photoelectron Spectroscopy." *Journal of Chemical Physics* 125(16): Art. No. 164315 (9 pages).

Zhang W, DE Culley, MA Gritsenko, RJ Moore, L Nie, H Scholten, K Petritis, EF Strittmatter, DG Camp II, RD Smith, and FJ Brockman. 2006. "LC-MS/MS-Based Proteomic Analysis and Functional Inference of Hypothetical Proteins in *Desulfovibrio vulgaris*." *Biochemical and Biophysical Research Communications* 349(4):1412-1419. doi:10.1016/j.bbrc.2006.09.019

Zhang Y, Y Song, F Yin, E Broderick, K Siegel, A Goddard, E Nieves, L Pasa-Tolic, Y Tanaka, H Wang, CT Morita, and E Oldfield. 2006. "Structural Studies of Vγ2Vδ2 T Cell Phosphoantigens." *Chemistry & Biology* 13(9):985-992.

Zhang Z, O Bondarchuk, BD Kay, JM White, and Z Dohnalek. 2006. "Imaging Water Dissociation on TiO_2(110): Evidence for Inequivalent Geminate OH Groups." *Journal of Physical Chemistry B* 110(43): 21840-21845.

Presentations

During this reporting period, EMSL staff presented on research performed at the user facility at the following meetings or locations.

- SPIE Conference, October 1-4, 2006, Boston, Massachusetts.
- Society of Exploration Geophysicists 76th Annual Meeting, October 1-6, 2006, New Orleans, Louisiana.
- Pennsylvania State University—PNNL Collaboration on Acid Mine Drainage Biogeochemistry and Biomineralization. Center for Environmental Kinetics Analysis, October 3, 2006, University Park, Pennsylvania.
- Fall 2006 Meeting of the Electrical Safety Improvement Project, October 10-11, 2006, Idaho Falls, Idaho.
- Neuroscience 2006 Conference, October 13-18, 2006, Atlanta, Georgia.
- Materials Science and Technology 2006 Conference and Exhibition, October 15-19, 2006, Cincinnati, Ohio.
- 62nd American Chemical Society Southwest Regional Meeting, October 19-22, 2006, Houston, Texas
- 21st Asilomar Conference on Mass Spectrometry, October 20-23, 2006, Pacific Grove, California.
- 53rd Annual Meeting of Radiation Research Society, November 4-9, 2006, Philadelphia, Pennsylvania.
- 4th International Congress on Electron Tomography, November 5-8, 2006, San Diego, California.
- HP-Cast Meeting, November, 10-11, 2006, Tampa, Florida.
- SuperComputing 06, November 11-17, 2006, Tampa, Florida.
- American Institute of Chemical Engineers 2006 Annual Meeting, November 12-17, 2006, San Francisco, California.
- American Vacuum Society 53rd International Symposium & Exhibition, November 12-17, 2006, San Francisco, California.
- 2006 Materials Research Society Fall Meeting, November 28-30, 2006, Boston, Massachusetts.
- 2006 Fall Meeting of the Materials Research Society, November 27-December 1, 2006, Boston, Massachusetts.

Patents

None reported

Journal Covers

The research of EMSL users Z Zhang, O Bondarchuk, BD Kay, JM White, and Z Dohnalek was featured on the cover of the November 2, 2006, issue of the *Journal of Physical Chemistry B*.

The research of EMSL users SA Chambers, TC Droubay, CM Wang, KM Rosso, SM Heald, DA Schwartz, KR Kittilstved, and DR Gamelin was featured in the November 2006 issue of *Materials Today*.